



**2004
SAVANNAH RIVER
COOLING TOWER
COLLECTION
(U)**



SRNL

SAVANNAH RIVER NATIONAL LABORATORY

We Put Science To Work

DISCLAIMER

This report was prepared as an account of work sponsored by an agency of the United States Government. Neither the United States Government nor any agency thereof, nor any of their employees, makes any warranty, express or implied, or assumes any legal liability or responsibility for the accuracy, completeness, or usefulness of any information, apparatus, product, or process disclosed, or represents that its use would not infringe privately owned rights. Reference herein to any specific commercial product, process or service by trade name, trademark, manufacture, or otherwise, does not necessarily constitute or imply its endorsement, recommendation, or favoring by the United States Government or any agency thereof. The views and opinions of authors expressed herein do not necessarily state or reflect those of the United States Government or any agency thereof.

2004
Savannah River Site
Cooling Tower Collection
(U)

Prepared by

Alfred J. Garrett, Matthew J. Parker, and E. Villa-Aleman
Atmospheric Technologies Group
Savannah River National Laboratory
Aiken, South Carolina, 29808

May 2005



Prepared for the US Department of Energy under contract No. DE-AC09-96SR18500

This page intentionally left blank.

ABSTRACT

The Savannah River National Laboratory (SRNL) collected ground truth in and around the Savannah River Site (SRS) F-Area cooling tower during the spring and summer of 2004. The ground truth data consisted of air temperatures and humidity inside and around the cooling tower, wind speed and direction, cooling water temperatures entering; inside and leaving the cooling tower, cooling tower fan exhaust velocities and thermal images taken from helicopters. The F-Area cooling tower had six cells, some of which were operated with fans off during long periods of the collection. The operating status (fan on or off) for each of the six cells was derived from operations logbooks and added to the collection database. SRNL collected the F-Area cooling tower data to produce a database suitable for validation of a cooling tower model used by one of SRNL's customer agencies. SRNL considers the data to be accurate enough for use in a model validation effort. Also, the thermal images of the cooling tower decks and throats combined with the temperature measurements inside the tower provide valuable information about the appearance of cooling towers as a function of fan operating status and time of day.

This page intentionally left blank.

TABLE OF CONTENTS

Abstract

<i>Introduction</i>	1
<i>Cooling Tower Description</i>	1
<i>Ground Data Collection</i>	4
<i>Ground Data Accuracy and Consistency</i>	5
<i>Measurements from Aircraft</i>	8
Figure 1. Schematic of Counter Flow Mechanical Draft Cooling Tower	2

LIST OF FIGURES

Figure 2. F-Area Cooling Tower	3
Figure 3. View of Cooling Tower from Deck Level	3
Figure 4. Cooling Water Falling from Fill into Basin	4
Figure 5. Onset Tidbit Temperature Sensor and HOBO Temperature and Humidity Sensor	5
Figure 6. HOBO Temperature and Humidity Sensor Suspended Inside Gap Between Drift Eliminators and Deck.....	5
Figure 7. Funnel Apparatus Designed to Capture Water Falling into Basin after Passing Through Fill	6
Figure 8. Fan Exhaust Velocities Close to Shroud	6
Figure 9. Fan Exhaust Velocities Away from Shroud	6
Figure 10. Individual Cells with Fans On.....	7
Figure 11. CT3 Water and Air Temps.....	8
Figure 12. Typical TidBit™ Calibration	9
Figure 13. HOBO Vs. Tidbit Cell 6 Air Temps	10
Figure 14. Computed Vs. Measured Exhaust Dewpoint Temperature from Cell 3.....	11
Figure 15. Water Vs. Air Measured Enthalpy Rate of Change in Cell 3	12

Figure 16. Thermal Image of F-Area Cooling Tower Cells Taken at an Elevation of
500 FT..... 14

Figure 17. Thermal Image of F-Area Cooling Tower Cells Taken at an Elevation of
300 FT..... 15

Figure 18. Thermal Image of F-Area Cooling Tower Cells Taken at an Elevation of
350 FT..... 16

Figure 19. Throat Vs. Deck: 4/27/04 Night..... 17

Figure 20. Throat Vs. Deck: 4/29/04 Day 17

INTRODUCTION

The Savannah River National Laboratory (SRNL) collected ground truth data in and around the cooling towers located in the Savannah River Site's (SRS) F-Area during the spring and summer of 2004. SRS is a 310 square mile nuclear facility in South Carolina operated by the US Department of Energy. F-Area is a former nuclear fuel reprocessing facility that was being prepared for permanent shutdown in 2004. For this reason, heat loads discharged by the F-Area mechanical draft cooling towers in 2004 were much less than the design specification heat loads. The F-Area cooling towers were often able to adequately cool water coming from the canyon building with some or all of the fans turned off. These low heat load, or "fans off" operating conditions were a key requirement for the collection, because cooling tower performance data for those off-normal conditions is not available in the open literature.

The objective of the F-Area cooling tower collection was acquisition of a data base suitable for validation of a cooling tower model used by one of SRNL's customer agencies. In addition to collection of cooling water temperatures, air temperatures and humidity inside and outside the cooling towers, SRNL collected airborne thermal imagery of the towers on three days and three nights.

The ground truth data collection consisted of air temperature and humidity measurements by sensors located in the cooling tower cells, water temperature measurements going into, coming out of and inside the cooling tower cells and ambient meteorological data. Cooling water flow rates and fan exhaust velocities were also measured. In addition, SRNL took thermal images of the cooling towers from helicopters on three days and three nights. These different measurements will be discussed in this report, along with analyses directed toward determining their consistency and accuracy.

COOLING TOWER DESCRIPTION

Figure 1 is a schematic of a counter flow mechanical draft cooling tower. There are three possible operating modes for a mechanical draft cooling tower: fans on with water circulating (normal operation), fans off with water circulating (natural convection mode), and fans off with no circulating water (shutdown). When the water is circulating, heated water enters near the top of the tower where it is sprayed evenly over the fill material. The fill is typically composed of many small rectangular or hexagonally shaped channels

Data
described
in
this
report
are
available
from
the
authors.

Schematic of Mechanical Draft Cooling Tower

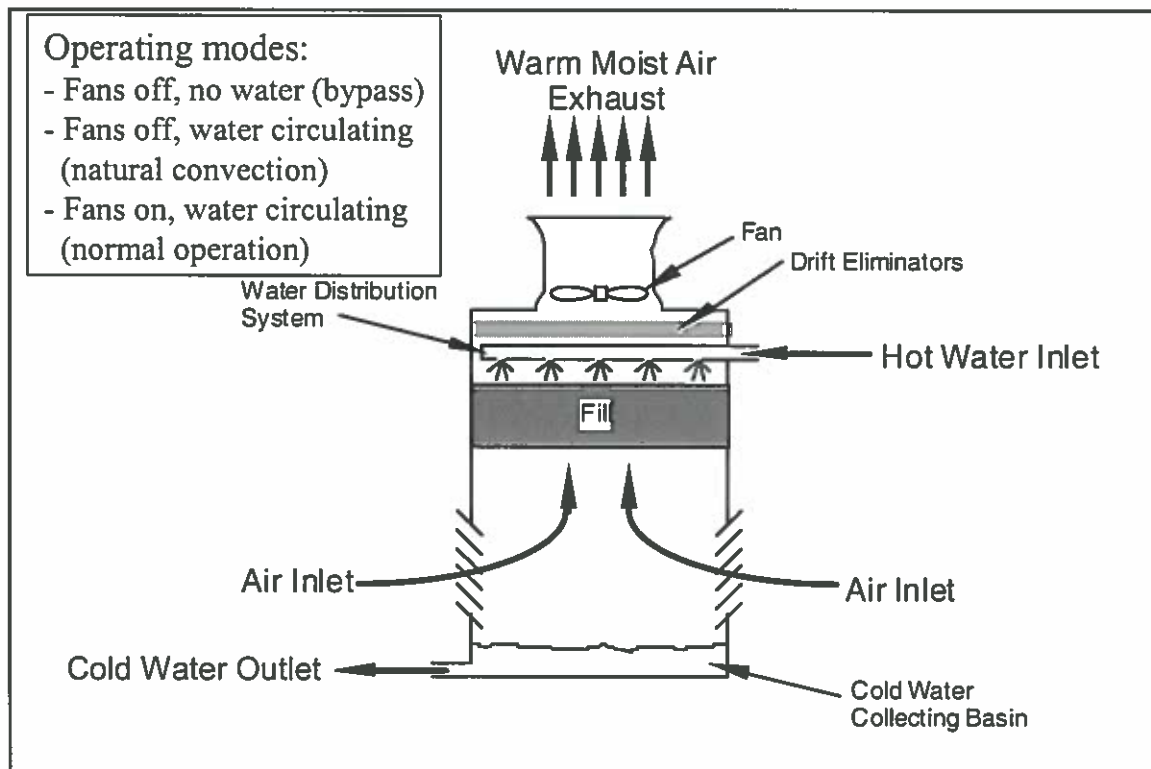


Figure 1: Schematic of counter flow mechanical draft cooling tower.

that are designed to create falling films of water, which maximize the contact of water with air flowing upward through the same channels. After passing through the fill, the water falls down to a basin at the bottom of the tower, where it combines with water from other cells and is pumped back to the process.

Figure 2 is a photograph of the F-Area counterflow cooling towers which were manufactured by the Marley Co. There are six cells which receive heated water from the F-Area canyon building from the same inlet line. Water that passes through the six cells is collected in a common basin and then flows back to the canyon building. The shrouds around the fans are 3.0 m high and have a diameter of 4.1 m (see Figure 3). The decks for each cell are approximately 8.5 m on a side and consist of a plastic matrix inside a metal grid. The deck is 10 m above ground level. Air flows into the cooling tower cells through slots on two sides. A metal barrier in the middle of each cell blocks airflow from coming in a slot on one side and passing out the other, so all inflowing air must go up through the tower fill and drift eliminators and out the fan exhaust at the top of each cell. Figure 4 shows water falling from the fill into the basin and the metal barrier in the background.

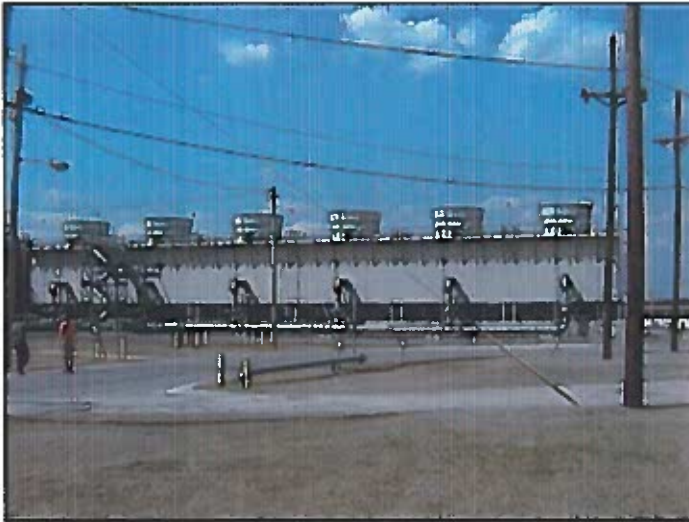


Figure 2: F-Area cooling tower. Pipes carrying heated water from the F-Area canyon building enter each cooling tower cell above air inflow slots at base of tower.

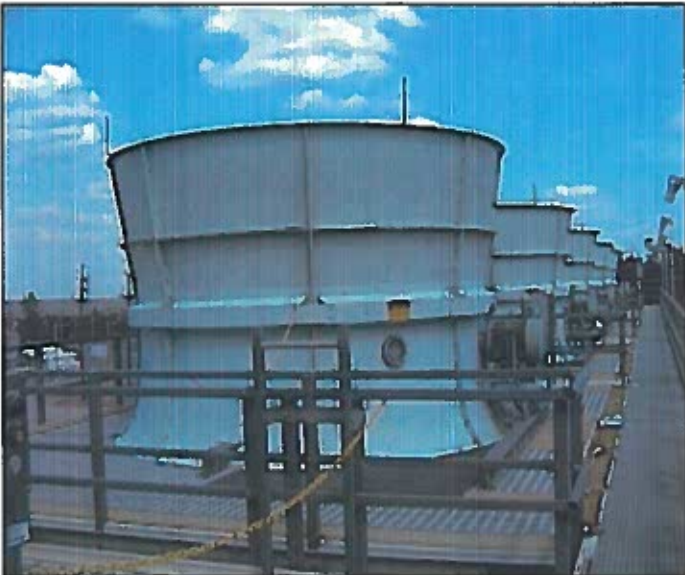


Figure 3: View of cooling tower cells from deck level. Deck material is a plastic matrix within a metal grid. Shroud directs fan exhaust upward.



Figure 4: Cooling water falling from fill into basin. Metal barrier that prevents wind from blowing through tower cells is in background.

GROUND DATA COLLECTION

Ground data collections inside and around the F-Area cooling tower cells started in late February 2004 and stopped early in August. Complete characterization of the air and water flow through the cooling towers required measurement of the following variables:

- Temperature and humidity of air entering and leaving cooling tower cells
- Temperature of water entering and leaving cooling tower cells.
- Cooling water flow rate
- Fan exhaust velocity (mass flow rate)
- Air pressure

The temperature and humidity of air being exhausted from the cooling tower were measured with Onset Computer Corporation HOBO® temperature and humidity sensors (Figure 5). Temperatures of water entering and leaving the cooling tower were measured with Stowaway Tidbit® sensors, also manufactured by Onset. Both the HOBO and Tidbit sensors are small, rugged sensors that contain their own battery operated data logging and storage, which allows these sensors to be permanently sealed and waterproof. Data are downloaded with non-invasion optical couplers. Tidbits and HOBO's were typically changed out every two weeks for data downloading, and this frequency also helped keep the humidity sensor from getting damaged due to prolonged exposure to saturated conditions.

HOBO's were placed inside the cooling tower cells between the drift eliminators and the deck (Figure 6). The photograph in Figure 6 was taken when the trap door entrance to the space between the drift eliminators and deck was open. When the trap door is closed, this space is sealed off from the ambient air, and the air temperature and humidity are the same as the exhaust air temperature and humidity.

The basin that collects water that has fallen through and been cooled by the six cells repre-



Figure 5: Onset Tidbit temperature sensor and HOBO temperature and humidity sensor.

sents an average exit cooling water temperature. In order to measure the performance of individual cooling tower cells, it was necessary to fabricate an apparatus that could temporarily capture water after it had passed through the fill, where most of the heat and mass transfer between water and air occurs, and before it reached the basin (Figure 7). The funnel apparatus in Figure 7 satisfied this need. A Tidbit was secured at the base of each of the funnels. The difference between inlet water temperature and Tidbit temperature in the funnel corresponded to the amount of cooling produced by the individual cooling tower cell. The funnel apparatus was not installed in all six cells until early May.

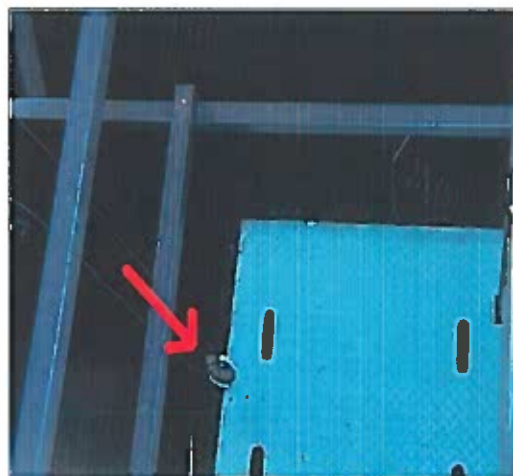


Figure 6: HOBO temperature and humidity sensor suspended inside gap between drift eliminators and deck.

Ambient air temperature, humidity and pressure were measured at the nearby SRS Central Climatology Station (CCS), which is a few kilometers south of F-Area. Air temperature and humidity were deemed to be reasonably representative of the conditions at the F-Area cooling tower facility given their close proximity. Minor differences can be expected under



Figure 7: Funnel apparatus designed to capture water falling into basin after passing through fill. A Tidbit was secured at the base of each of the funnels. The difference between the inlet water temperature and the Tidbit temperature in the funnel was the amount of cooling produced by the individual cooling tower cell.

daytime conditions when the F-Area building complex was likely to be slightly warmer and drier (lower dew points).

Fan exhaust velocities were spot measured with a portable anemometer above cells with running fans near the edge of the shroud (Figure 8) and midway between the shroud and the center of the fan (Figure 9). The average exhaust velocity near the shroud was 8.5 m/s, and

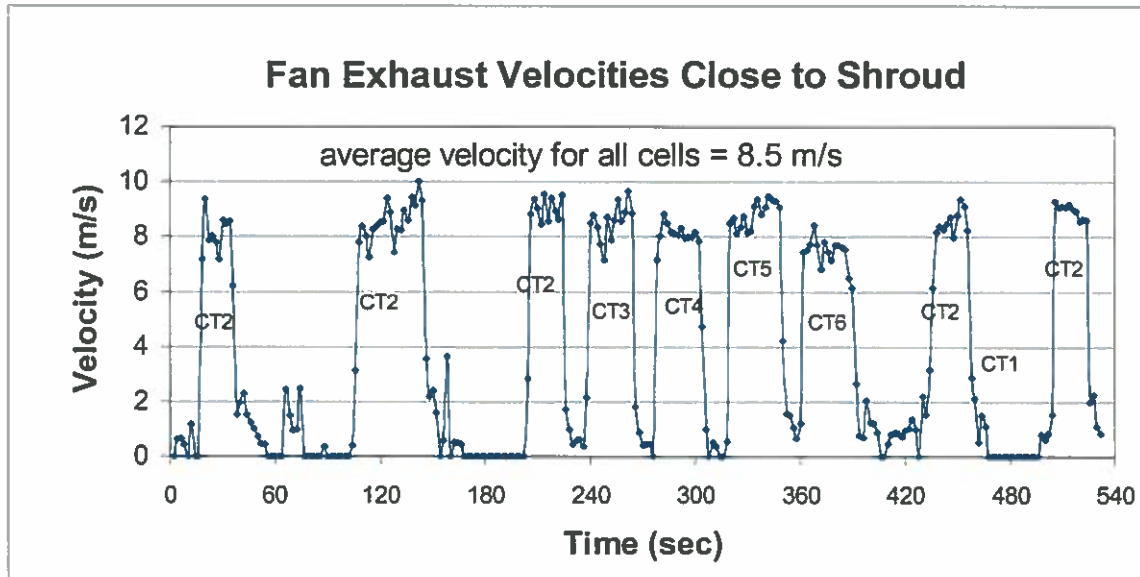


Figure 8: Measured velocities over exhaust fans close to shroud from the five F-Area cooling tower cells with fans on.

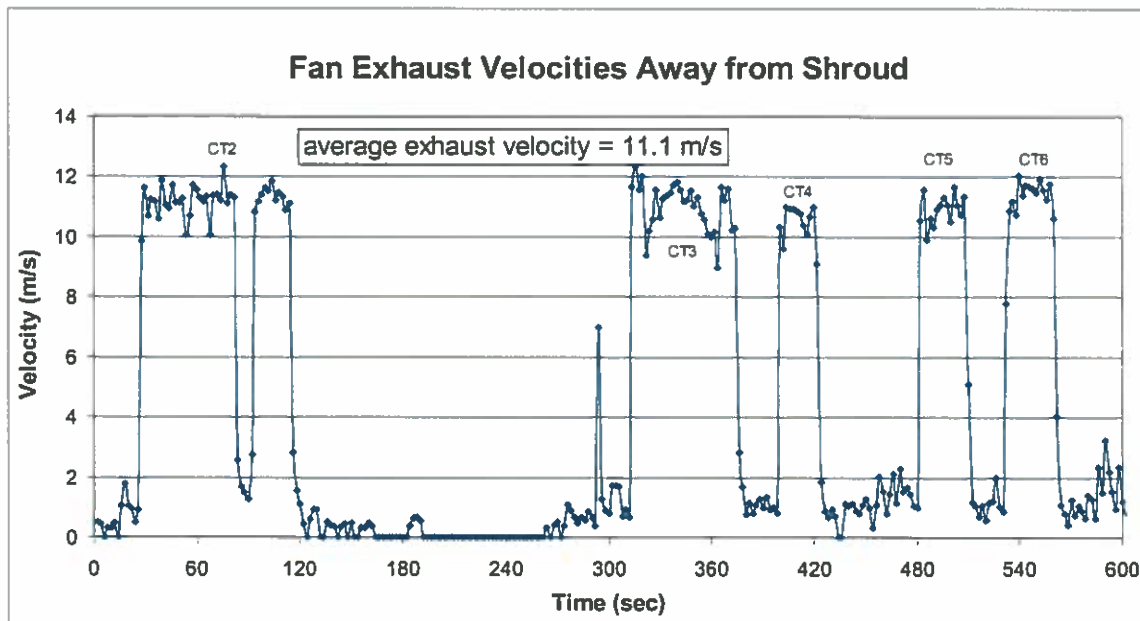


Figure 9: Measured velocities over exhaust fans midway between shroud and center of fans for the five cells with fans on.

the average midway velocity was 11.1 m/s. The lower velocity near the shroud is probably the result of the combined effect of frictional drag from the shroud and the gap between the end of the fan blades and the shroud where no upward thrust was being generated. The velocities are almost certainly lower near the center of the fan, where fan blade angular velocities are lower. For these reasons, the average exhaust velocity for the entire area inside the shroud is estimated to be 10.0 m/s with an uncertainty of +/- 1.0 m/s. These measurements were made with an Extech Instruments #451126 anemometer. The fan velocities shown in Figures 8 and 9 represent the flow generated when fans are at 100% normal rpm and are considered to be very representative of normal operating conditions. It is also possible to run the fans at 50% rpm, but this was rarely observed.

Figure 10 shows the fan status for the six cells during the 2004 collection period. Since the heat loads from the F-Area Canyon were low, it was not necessary to turn the fans on until the advent of warmer, more humid weather in May. The fan in Cell 1 was never turned on during the collection period. Figure 10 is based on data taken from the F-Area Operations logsheets. Fan status was recorded three times a day (once per shift). For this reason, there were periods of a few hours for Cells 2 through 6 when the fan status is not known and were inferred from the measurements. These instances were infrequent, because as Figure 10 shows, Cell 1 was never on, and the other five cells were on continuously from May through the end of the collection in early August. SRNL attempted to measure the fan exhaust velocity above Cell 1, (see Figure 8), but the portable anemometer was not sensitive enough to measure the weak exhaust velocities at that time.

Cooling water flow rates during the 2004 collection were historically low relative to the

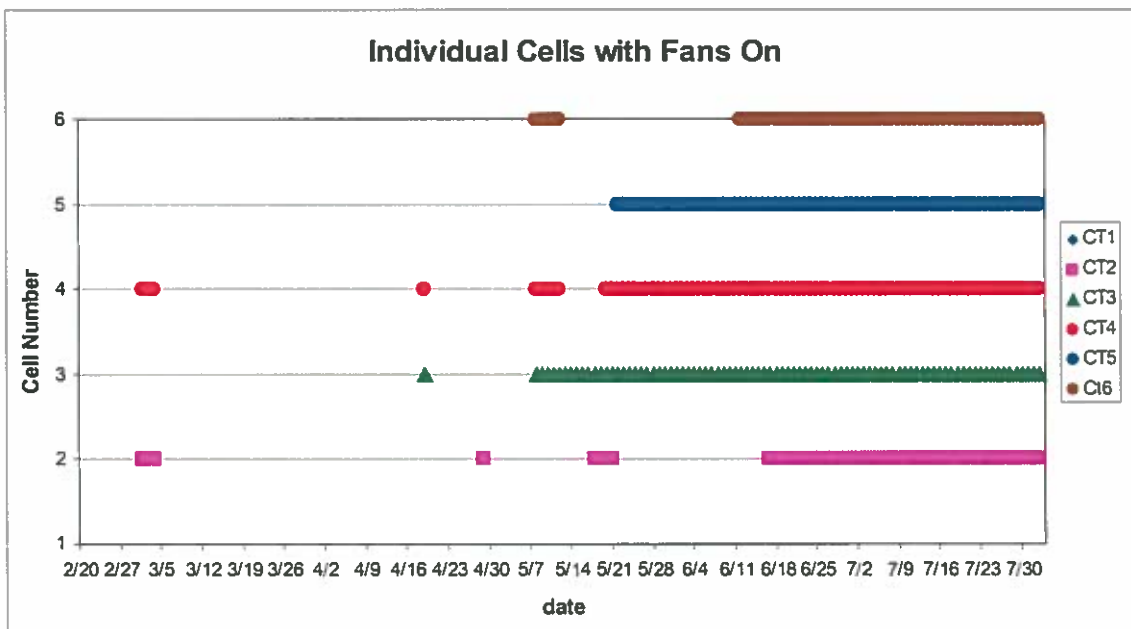


Figure 10: Operating status of F-Area cooling tower fans during collection period. Colored symbols indicate when fans were on.

flow rate when irradiated nuclear fuel was being reprocessed in F-Canyon in years past. SRNL measured a flow rate of 4200 gpm (265 liters/second) during the collection period, or 700 gpm per cell. SRNL made the flow measurement with a paddlewheel flowmeter at 20 locations on a grid with evenly intervals across and down into the rectangular discharge channel from the tower basin. The uncertainty of the 4200 gpm measurement was estimated to be +/- 200 gpm, or about 5%.

Figure 11 is a plot of temperature variables measured in Cell 3 in late May. This figure illustrates some of the relationships between different temperatures over a three day period. In Figure 11, Tamb is the ambient air temperature, Tambdew is the ambient dewpoint temperature, Airexhaust is the exhaust air temperature from Cell 3, Dewptexhaust is the dewpoint temperature of the exhaust air, Cwinlet is the inlet cooling water temperature (common to all six cells), ctshower is the water temperature after it has flowed through the Cell 3 fill and has fallen to a level just above the basin, where its temperature was measured using the apparatus shown in Figure 5. It can be seen in Figure 11 that the exhaust air temperature tracked the ambient air temperature, but was always cooler except right at dawn on the first two days, when Tamb was lowest and cwinlet was high enough to warm the air passing through the tower above Tamb. During the day, Airexhaust was often warmer than cwinlet, indicating that heat was actually being transferred from the air to the cooler water, which is not typical. However, ctshower was almost always lower than cwinlet, so some cooling of the water was occurring at just about all times. It can be concluded that evaporative cooling dominated over sensible heat transfer. This was clearly the case, because Tambdew was always lower than Dewptexhaust, which means that heat was extracted from the

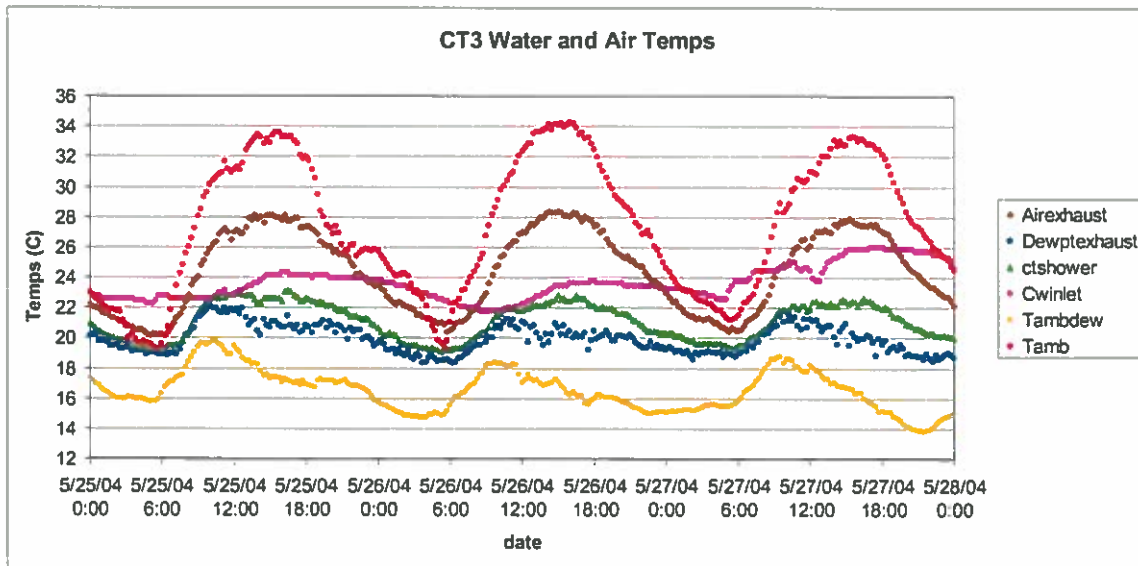


Figure 11: Relationships between cooling water inlet temperature (Cwinlet), ambient air temperature (Tamb), ambient dewpoint temperature (Tambdew), water temperature exiting Cell 3 (ctshower), air temperature exiting Cell 3 (Airexhaust) and dewpoint temperature of air exiting Cell 3 (Dewptexhaust).

air to supply the latent heat of vaporization.

Data files have been created for each of the six cells that contain the variables shown in Figure 11, plus the following variables: air exhaust measured by Tidbit (redundant measurement), basin exit temperature, ambient air pressure and fan status (on/off). Measurements were recorded every 15 minutes. The data files start on April 27, 2004 and end on August 2, 2004. These data files are available (along with this report) to qualified users approved by the agency that funded this data collection.

GROUND DATA ACCURACY AND CONSISTENCY

Onset Computer claims an accuracy of 0.2°C absolute accuracy for its Tidbit temperature sensors, within the specified calibration range of the sensor. SRNL has performed many calibration checks on the Tidbits, and has verified the accuracy claimed by Onset Computer (Figure 12). During the 2004 F-Area collection, SRNL put a Tidbit and a HOBO in the space between the drift eliminators and the cooling tower deck. Figure 13 compares the independent temperature measurements made by these two sensors for Cell 6 for the month of June, 2004. It can be seen that the two temperature time series are nearly identical. For the entire collection period (May 10 to August 2) the average temperatures measured by the two sensors differed by only 0.01°C.

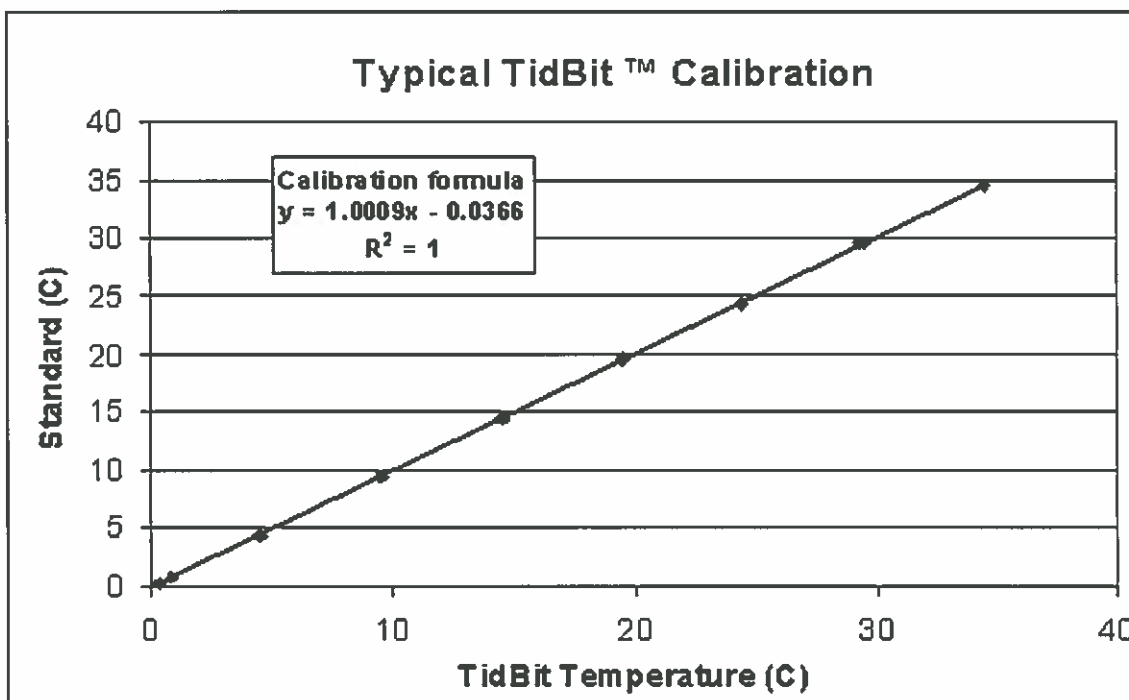


Figure 12: Example of Tidbit temperature sensor calibration check that verifies manufacturer's (Onset Computer) claim of 0.2°C accuracy.

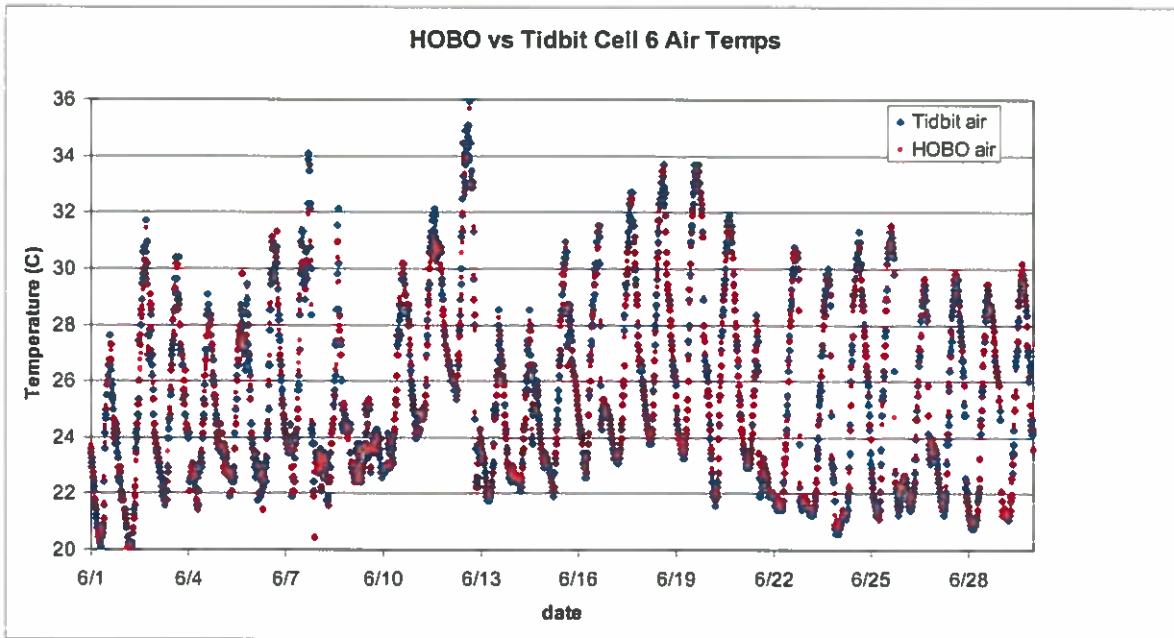


Figure 13: Comparison of air temperatures measured by Tidbit and HOBO sensors inside Cell 6 for month of June 2004. Average temperatures for entire collection period differed by only 0.01° C.

HOBO's also measure humidity, which is more difficult to measure accurately than temperature. In its user's manual Onset notes that the HOBO humidity sensor can become saturated and give erroneously high humidity measurements when they are left in a humid environment for long periods of time. SRNL attempted to determine if there were significant humidity measurement errors by using the balance between the enthalpy lost by the cooling water as it passed through the cooling tower cells and the enthalpy gained by the air flowing through the cells. The equations used to compute the water and air enthalpies are shown in the adjacent box.

Equation 1 expresses the equality between the total air plus water enthalpy entering the cooling tower cell (H_{ai} and H_{wi}) and the total enthalpy leaving the cooling tower cell (H_{ao} and H_{wo}). The variables in Equation 1 are actually time rates of change of enthalpy, and have units of cal/s, but will be referred to as enthalpies for brevity.

$$\begin{aligned}
 H_{ai} + H_{wi} &= H_{ao} + H_{wo} & (1) \\
 H_{ai} &= c_{pa} T_{ai} F_{ai} + L q_{ai} F_{ai} & (2) \\
 H_{wi} &= c_{pw} T_{wi} F_{wi} & (3) \\
 H_{ao} &= c_{pa} T_{ao} F_{ao} + L q_{ao} F_{ao} & (4) \\
 H_{wo} &= c_{pw} T_{wo} F_{wo} & (5) \\
 F_{ai} &= \pi R_{twr}^2 w \rho_{ad} (1 + q_{ai}) & (6) \\
 F_{ao} &= \pi R_{twr}^2 w \rho_{ad} (1 + q_{ao}) & (7) \\
 F_{wo} &= F_{wi} - \pi R_{twr}^2 w \rho_{ad} (q_{ao} - q_{ai}) & (8)
 \end{aligned}$$

Equations 2 and 4 define the entering and exiting air enthalpies, which have a sensible heat component and a latent heat component. c_{pa} is specific heat of air, T_{ai} and T_{ao} are entering and exiting air temperatures, F_{ai} and F_{ao} are entering and exiting air mass flow rates in gm/s, L is heat of condensation for water vapor (cal/gm) and q_{ai} and q_{ao} are the dimensionless specific humidity of the entering and exiting air (gm water vapor per gm of dry air). Equations 3 and 5 define the entering and exiting water enthalpies, in which c_{pw} is the specific heat of water, T_{wi} and T_{wo} are the entering and exiting water temperatures and F_{wi} and F_{wo} are the entering and exiting water flow rates (gm/s). Equations 6 and 7 define the entering and exiting air flow rates, in which R_{lwr} is the shroud diameter, w is the average exhaust velocity over the area inside the shroud and ρ_{ad} is the density of dry air (gm/m^3). The entering water flow rate F_{wi} is a measured quantity and the difference between it and the water flow rate exiting the cell (F_{wo}) is defined in Equation 8. As a practical matter, the differences between F_{ao} and F_{ai} , and F_{wo} and F_{wi} are much smaller than the measurement uncertainty of the air and water flows, so they are assumed to be equal in the enthalpy balance calculations discussed next. Also, the difference between the density of dry and moist air is neglected in these calculations.

The check on the accuracy of the HOBO humidity measurements, besides spot checks against a traceable standard before deployment, was done in terms of dewpoint temperature, which can be computed from specific humidity, air temperature and air pressure. Cooling tower Cell 3 was chosen for the test, because its fans were on during the entire data collec-

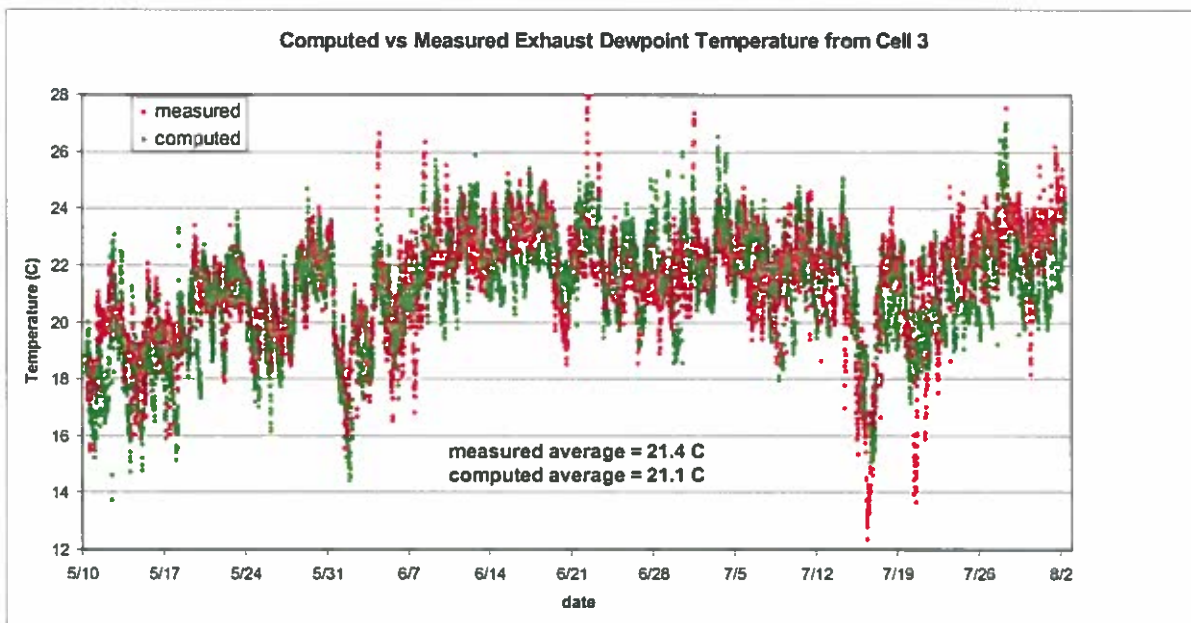


Figure 14: Comparison of measured and computed dewpoint temperatures for Cell 3. Computed values were found by assuming equality between enthalpy lost by cooling water passing through cell and enthalpy gained by air flowing through the cell.

tion, and therefore the fan exhaust velocity (10 m/s) was known. Given the measured air exhaust velocity, all variables in Equations (1) – (8) are known, and it is possible to compute a given variable as a residual and then compare the computed to the measured values. Figure 14 is a time series plot of the computed and measured dewpoint temperatures for Cell 3. In general, there is good agreement between the computed and measured values of dewpoint temperature, with an average difference of only 0.3°C. However, there are periods when the difference is larger. The average measured dewpoint temperature is slightly larger, which is the expected result, given that the HOBO's have a tendency to saturate and produce dewpoint temperatures larger than the true values if the sensor has been in an extremely moist environment for a long time. It should be noted that typical regulatory standard guidance requires dew point measurement accuracy to $\pm 1.5^\circ\text{C}$, so the assessed difference of 0.3°C is well within this range.

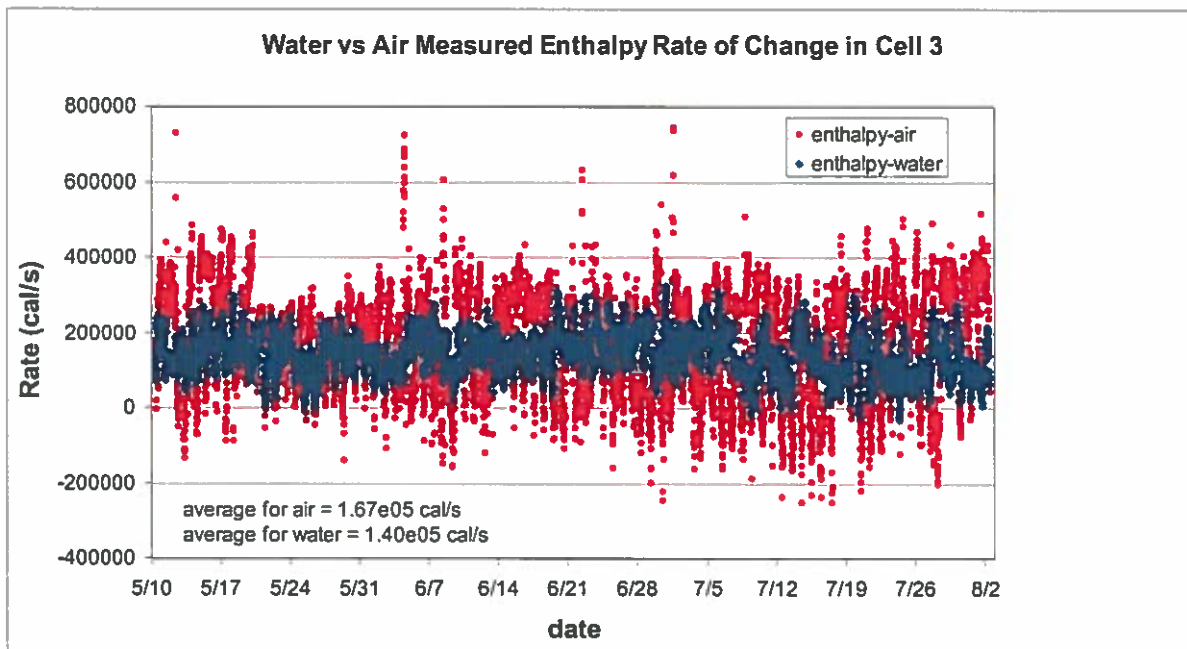


Figure 15: Comparison of computed rates of change in enthalpy of cooling water and air flow through Cell 3 based on measured flow rates, temperatures and dewpoints.

Figure 15 is a plot of the rates at which sensible and latent energy (enthalpy) was exchanged between the Cell 3 cooling water and air flows. These rates of enthalpy transfer have units of cal/s, and are based on the measured air and dewpoint temperatures inside and outside the cooling tower, plus the measured cooling water and airflow rates inside the tower. The average rate of change of enthalpy from the air data is 1.67e05 cal/s, versus 1.40e05 cal/s for the water, which is a difference of about 20%. As noted in the discussion of Figure 14, a 0.3°C increase in the ambient dewpoint temperature or an equal decrease in the Cell 3 exhaust dewpoint temperature would bring the two computed enthalpies into agreement. A 0.6°C

increase in the ambient air temperature or an equal decrease in the Cell 2 exhaust air temperature would also bring the two enthalpies into agreement. Measurement errors of 0.3 to 0.6°C could easily have been caused by sensor calibration uncertainties at CCS, unrepresentative data from CCS because it was several kilometers away from F-Area, unrepresentative measurements inside Cell 3 caused by maldistribution of cooling water in the fill or incomplete mixing of air in the space between the drift eliminators and the cooling tower deck. The cooling water and air flow rate measurements were probably accurate to no more than +/- 10%, so errors in those measurements could also have contributed to the 20% difference between the average rates of change in enthalpies.

The diurnal variation in the air enthalpy rate of change in Figure 15 is much greater than the water enthalpy rate of change. Since the water temperatures were all measured by Tidbits, which have a 0.2°C absolute temperature measurement accuracy, it appears that the air enthalpies are probably the source of the errors leading to the differences between the two enthalpies shown in Figure 15. The diurnal range in ambient and Cell 3 air temperatures was typically 10 to 15°C (see Figure 11), so errors on the order of 1.0°C that would have amplified the diurnal range of the computed air enthalpy rate of change may exist in the data and not be apparent. Those errors would probably be a combination of actual sensor error and sampling error (biases introduced by a sensor location that is not representative of area-averaged air temperatures).

The calibration, redundancy checks and enthalpy balance checks all lead to the conclusion that the 2004 F-Area cooling tower collection data can be used for analysis of cooling tower operations under low-heat load conditions, both for the fans on and for the fans off cases. These data are therefore also appropriate for model validation, with the following qualifications. For validation of a model's ability to correctly predict cooling water temperature drop based on inlet water temperature, cooling water flow rate and ambient temperature and dewpoint, these measurements should be highly reliable, because the Tidbit water temperature measurements have a +/- 0.2°C accuracy and these calculations are fairly insensitive to errors in ambient air and dewpoint temperature measurements (used to compute wetbulb temperature). For model validation which uses cooling tower throat temperature measurements, the uncertainties in the exhaust dewpoint temperature enter the analysis because this validation method relies on a balance between air and water enthalpy rate of change. The uncertainties in the enthalpy balance were discussed in the previous paragraphs of this section. Figure 15 implies that on the average, a model validation that uses an enthalpy balance can be fairly accurate, but individual estimates of heat dissipation rates may have significant errors.

MEASUREMENT FROM AIRCRAFT

In addition to the ground-based measurements, SRNL also took thermal images of the F-Area cooling tower cells from helicopters provided by Wackenhut (site security) on three

days (April 27 at 1430 and 2220 local time, April 29 at 1420 and 2220 local time, May 19 at 1540 local time and May 20 at 0200 local time). SRNL took thermal images at several elevations during each of the six aerial collections. The purpose of the aerial collections was to collect thermal imagery of the cooling tower cell deck and throat (region inside shroud).

Along with the thermal images, emissivity measurements of the throat and deck were needed to convert the radiances measured by the thermal camera to temperatures. Solar absorptivity measurements were needed as inputs to the cooling tower model that computes thermal energy dissipation rates from cooling tower images. The instrument used for these measurements was a TESA 2000 –Total Emittance/Solar Absorptance portable reflectometer, manufactured by AZ Technology. This single instrument allows for the measurement of surface properties in both the infrared and solar regions. The wavelength range is $3\mu\text{m}$ to $35\mu\text{m}$ in the thermal emissivity mode and $0.25\mu\text{m}$ to $2.5\mu\text{m}$ in the solar absorptance mode. The portable nature of the instrument allows for field measurement without the need for taking samples back to the lab, which in many cases would damage the target. Also in-situ measurements are desired for targets such as soils since the surface properties are altered when disturbed and taken to the lab for measurements.

Solid surfaces inside the shroud include the fan blades, supporting structures for the fans and the drift eliminators, which consist of a honeycomb-like plastic matrix with diamond-shaped cell diameters of about 3 cm. The 3 m height of the shroud prevented measurement

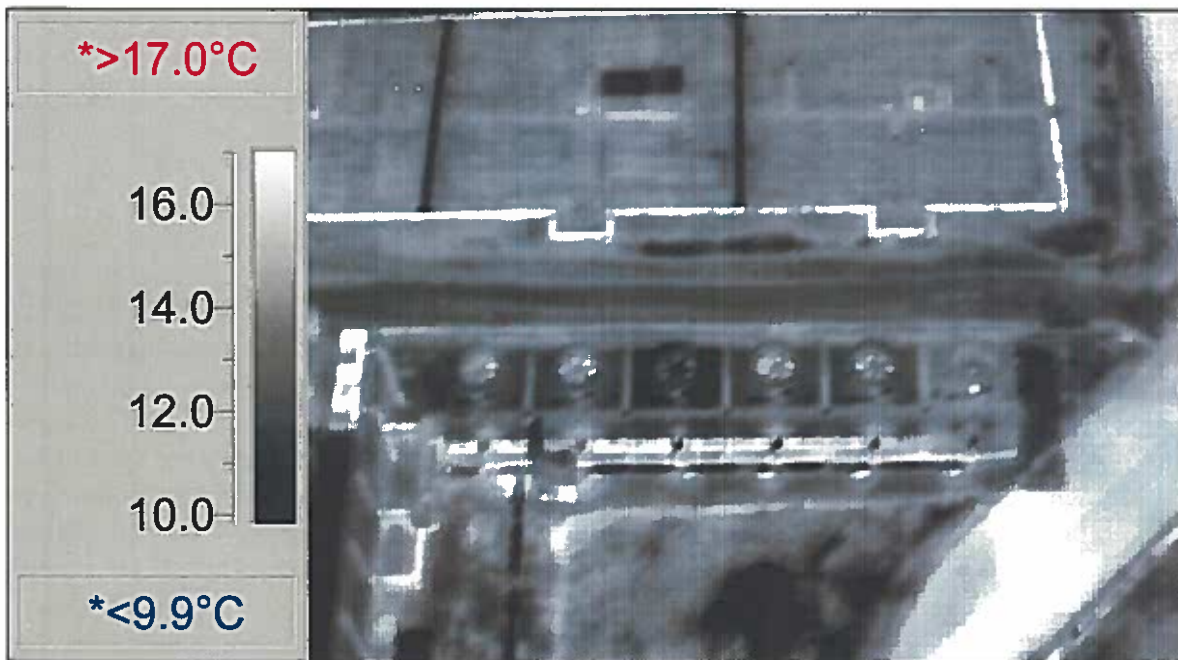


Figure 16: Thermal image of F-Area cooling tower cells taken at an elevation of 500 ft (150 m) at 2218 local time on April 27. From left to right, Cell 3 was in bypass mode (water and fans off), Cell 6 was fully operational (fans and water on); all other cells had water flow but fans off. Temperature scale based on assumed emissivity of 1.0.

of the emissivity and solar absorptivity of the surfaces inside the throat. The decks were primarily plastic squares embedded in a metallic grid (see Figure 3). Both the plastic and metal surfaces have a measured emissivity of 0.98. The solar absorptivities of the plastic and metal surfaces were 0.78 and 0.66, respectively, which gives an area-weighted solar absorptivity for the deck surface of 0.74. The solar absorptivity of the outer surface of the shroud is 0.52 and its emissivity is 0.95.

Figure 17 is a thermal image of F-Area cooling tower cells taken at an elevation of 300 ft



Figure 17: Thermal image of F-Area cooling tower cells taken at an elevation of 300 ft (90 m) at 2213 local time on April 27. Cells 3 was in bypass mode (water and fans off), Cell 6 was fully operational (fans and water on); all other cells had water flow but fans off. Temperature scale based on assumed emissivity of 1.0.

(90 m) at 2213 local time on April 27. Cells 3 was in bypass mode (water and fans off), Cell 6 was fully operational (fans and water on); all other cells had water flow but fans off. At this elevation, some of the structures underneath the fan blades inside the shroud are resolved. The hot motor at the base of the shroud and the gear box in the middle of the throat in Cell 6 can be clearly seen. The moving fan blades in Cell 6 cannot be seen because the time the thermal camera took to make the image was long relative to the time it took for the blades to rotate. Note that the throat in Cell 6 was cooler than the throats in Cells 4 and 5 because the larger amount of heat removed from the cooling water passing through Cell 6 was distributed in a much greater volume of air. The deck of Cell 6 was warmer than the decks of Cells 4 and 5 because there was better heat transfer from the rapidly moving, turbulent air beneath the deck to the lower surface of the deck.

Figure 18 is a thermal image of F-Area cooling tower cells taken at an elevation of 350 feet

(105 m) at 1410 local time on April 29. Strong solar heating masked the thermal signal from all cells except for Cell 2, which had fans on. The much better heat transfer from the air beneath the deck to the lower surface of the deck in Cell 2 kept the upper surface of the deck much cooler than the decks of cells with fans off. This was also the case for the surfaces inside the throat. In this daytime case, the much more efficient heat transfer produced by the fans removed much of the solar heating in addition to more heat from the cooling water passing through the cell. Collectively, Figures 16, 17 and 18 show that interpretation of cooling tower operating status from thermal imagery must be done with an understanding of the dynamics and thermodynamics at work at a given time, because the warmest cells are not necessarily the ones removing the largest amount of heat from the cooling water. Figure 19 shows computed cooling tower throat and deck temperatures derived from the

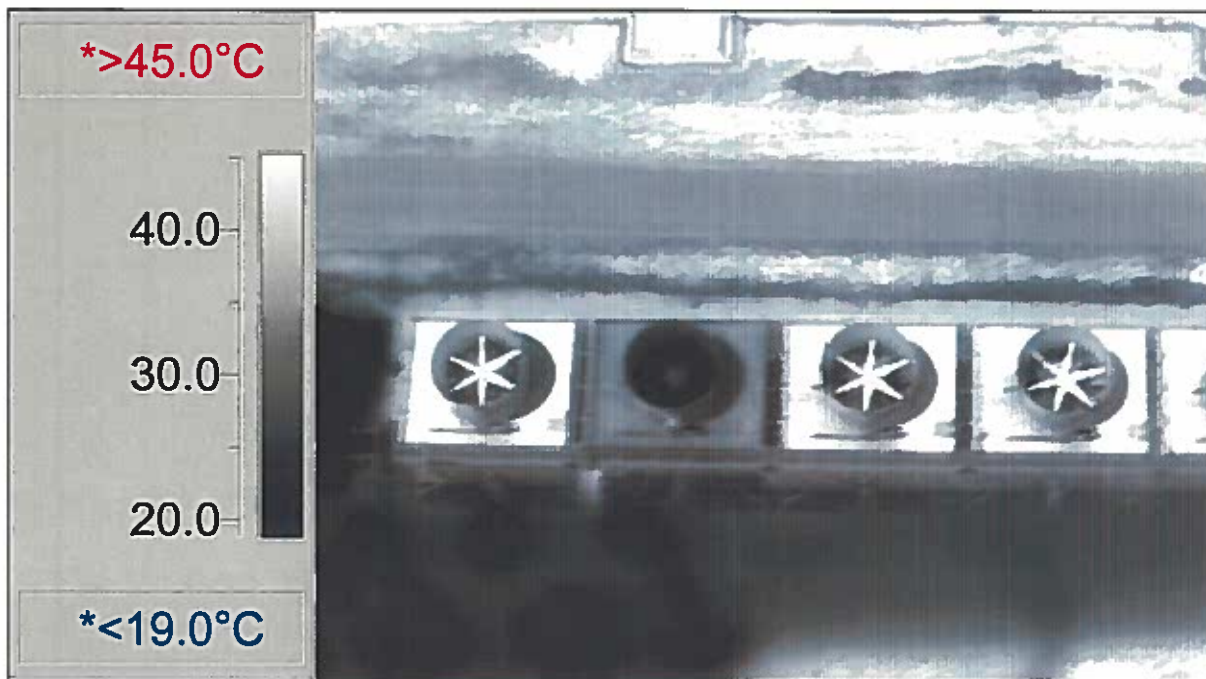


Figure 18: Thermal image of F-Area cooling tower cells taken at an elevation of 350 feet (105 m) at 1410 local time on April 29. Strong solar heating masked the thermal signal from all cells except for Cell 2, which had fans on.

thermal image shown in Figure 15, which was taken late at night on April 27. Cells 1, 2, 4 and 5 had water circulating but fans off, Cell 3 was in bypass mode and Cell 6 had fans on. The emissivity was assumed to be 1.0 in all cases. Cell 3 was significantly colder than the other cells, but the differences between the deck and throat temperatures of Cell 6 and the cells with fans off but water circulating were not large, even though their appearance in the thermal image was quite different. The deck and throat temperatures in Cell 6 were much closer to each other because the higher air flow and better heat transfer raised the deck temperature but lowered the throat temperature because the heat drawn from the cooling water

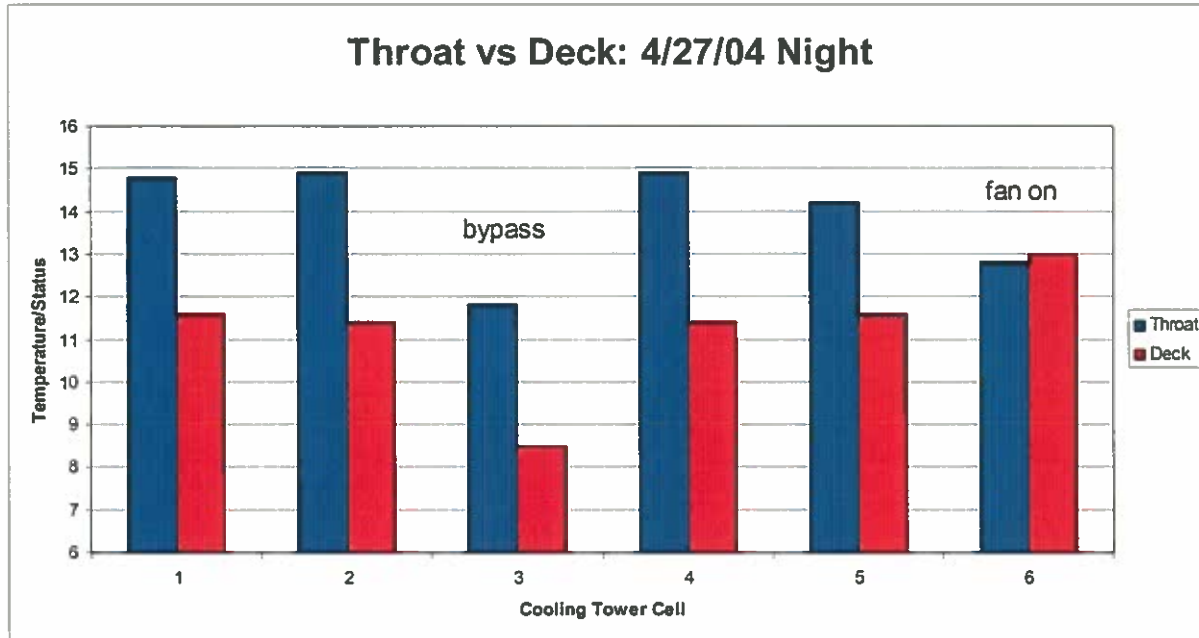


Figure 19: Cooling tower throat and deck temperatures derived from thermal image shown in Figure 16 (night, April 27). Cells 1, 2, 4 and 5 had water circulating but fans off, Cell 3 was in bypass mode and Cell 6 had fans on. Emissivity was assumed to be 1.0 in all cases.

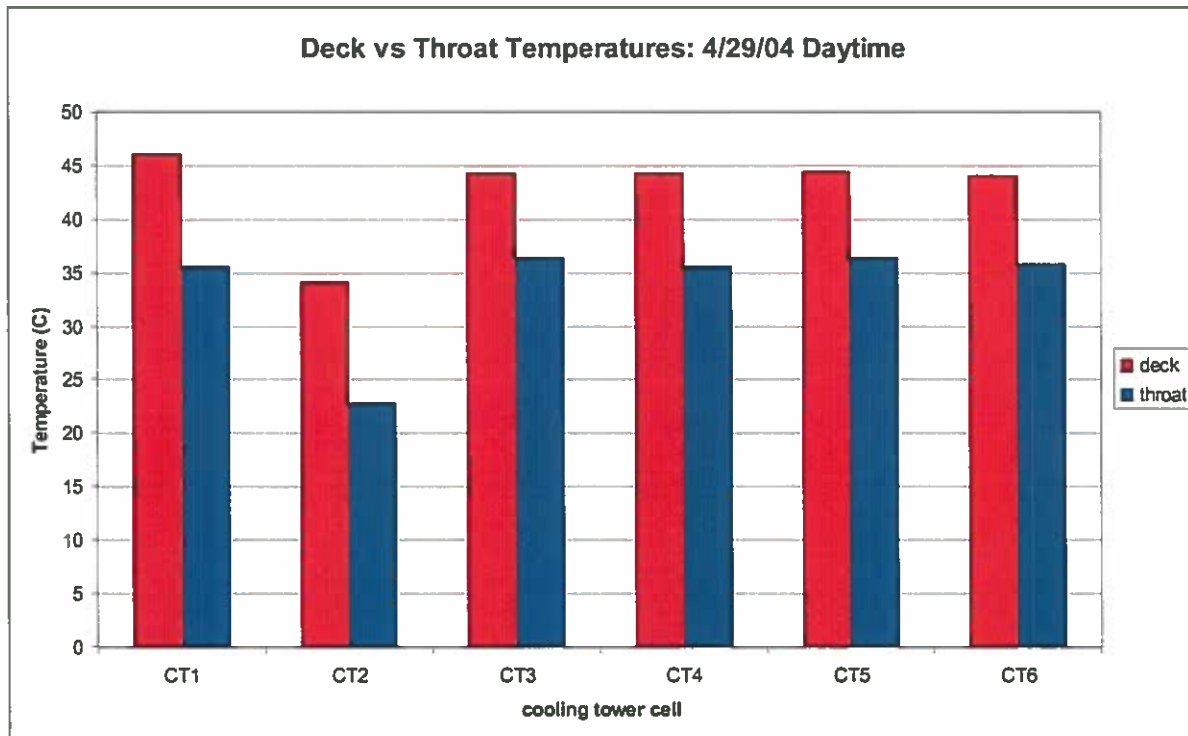


Figure 20: Cooling tower deck temperatures derived from thermal image shown in Figure 18 (early afternoon, April 29). Cell 2 had fans on, Cells 1, 3, 5 and 6 had water circulating but fans off, Cell 4 was in bypass mode.

was transferred to a large volume of air relative to the cells with fans off.

Figure 20 shows cooling tower deck temperatures derived from the thermal image shown in Figure 18, which was taken early in the afternoon of April 29. Cell 2 had fans on, Cells 1, 3, 5 and 6 had water circulating but fans off and Cell 4 was in bypass mode. Both the deck and the throat of Cell 2 were approximately 10°C colder than their counterparts in the other cells. Cell 4 temperatures were indistinguishable from the cells with water circulating but fans off, because the small amount of heat supplied to the throat exhaust air by the cooling water was insignificant relative to the strong solar heating on all exposed surfaces.

AUTHOR CONTACT INFORMATION

Alfred J. Garrett

Nonproliferation Technologies Section
Savannah River National Laboratory
Bldg. 7735-A
Aiken, SC 29808
Phone: 803-725-4870
Email: alfred.garrett@srnl.doe.gov

Matthew J. Parker

Nonproliferation Technologies Section
Savannah River National Laboratory
Bldg. 735-7A
Aiken, SC 29808
Phone: 803-725-2805
Email: matt.parker@srnl.doe.gov

Eliel Villa-Aleman

Nonproliferation Technologies Section
Savannah River National Laboratory
Bldg. 735-7A
Aiken, SC 29808
Phone: 803-725-0845
Email: eliel.villa-aleman@srnl.doe.gov

DISTRIBUTION

A. L. Boni, 773-A
A. J. Garrett, 735-A
R. P. Addis, 773-A
R. J. Kurzeja, 773-A
M. J. Parker, 735-7A
E. Villa-Aleman, 735A

ATG files (15), 773-A



